Design and Functional Evaluation of a Quasi-Passive Compliant Stance Control Knee–Ankle–Foot Orthosis

Kamran Shamaei, *Student Member, IEEE*, Paul C. Napolitano, and Aaron M. Dollar, *Senior Member, IEEE*

***Abstract*—In this paper, we present the mechanical design, control algorithm, and functional evaluation of a quasi-passive compliant stance control knee–ankle–foot orthosis. The orthosis implements a spring in parallel with the knee joint during the stance phase of the gait and allows free rotation during the swing phase. The design is inspired by the moment-angle analysis of the knee joint revealing that the knee function approximates that of a linear torsional spring in the stance phase of the gait. Our orthosis aims to restore the natural function of a knee that is impaired by injury, stroke, post-polio, multiple sclerosis, spinal cord injury, patellofemoral pain syndrome, osteoarthritis, and others. Compared with state-of-the-art stance control orthoses, which rigidly lock the knee during the stance phase, the described orthosis intends to provide the natural shock absorption function of the knee in order to reduce compensatory movements both in the affected and unaffected limbs. Preliminary testing on three unimpaired subjects showed that compliant support of the knee provided by the orthosis explained here results in higher gait speed as well as more natural kinematic profiles for the lower extremities when compared with rigid support of the knee provided by an advanced commercial stance control orthosis.**

***Index Terms*—Compliant mechanism, knee, knee–ankle–foot orthosis (KAFO), orthotics, quasi-passive mechanism, quasi-stiffness, spinal cord injury, stance control orthosis, stroke.**

Fig. 1. Quasi-passive compliant stance control orthosis lateral view without a shoe and frontal view with a shoe.

I. Introduction

THOUSANDS of patients suffer from knee instability as a result of impaired quadriceps following injury, stroke, post-polio, multiple sclerosis, spinal cord injury (SCI), patellofemoral pain syndrome, osteoarthritis, and others [1]–[5]. Traditionally, the affected knee is supported during walking using a knee–ankle–foot orthosis (KAFO), comprising a rigid thermoplastic cast formed around the impaired leg, as described in [6]. Traditional KAFOs lock the knee throughout the gait, and therefore require compensatory, unnatural, and metabolically expensive movements including circumducting on the braced leg, vaulting on the contralateral leg, swing phase hip elevation, and lateral sway in the upper body [7]–[11]. Those problems have led to a high rate (more than 60%) of abandonment of KAFOs [12]–[14].

Stance control KAFOs (SCKAFOs) have recently been commercialized and used clinically for patients with paresis and paralysis in the lower limb muscles [4], [7]–[10], [12], [14]–[29]. Unlike traditional KAFOs, SCKAFOs actively lock the knee only during the stance phase and allow for free rotation during the swing phase. This improvement has led to many medical benefits, including increased walking speed, knee range of motion, stride, step lengths, user satisfaction, reduced energy expenditure and gait asymmetry, as well as kinematic benefits to both affected and unaffected legs, compared with regular KAFOs [7]–[9], [20], [23]. However, rigid locking of the knee joint during stance phase in current SCKAFOs hinders the shock absorbing flexion of the knee (as outlined in [30], [31]), and can potentially cause increased metabolic cost, user pain and discomfort and limited gait speed. To overcome these issues, SCKAFOs can implement compliant support (instead of rigid locking) in the stance phase to replicate the damping

Manuscript received April 01, 2013; revised September 09, 2013 and December 13, 2013; accepted February 07, 2014. Date of publication February 19, 2014; date of current version March 05, 2014. This work was supported by the U.S. Defense Medical Research Development Program under Grant W81XWH-11-2-0054.

The authors are with the Department of Mechanical Engineering and Materials Science, Yale University, New Haven, CT 06511 USA (e-mail: kamran.shamaei@yale.edu; paul.napolitano@yale.edu; aaron.dollar@yale.edu).

Color versions of one or more of the figures in this paper are available online at http://ieeexplore.ieee.org.

Digital Object Identifier 10.1109/TNSRE.2014.2305664

function of the knee during stance [32]. Previous research on the moment-angle performance of the knee reveals that this joint behaves close to a linear torsional spring in the stance phase at the preferred gait speed; a spring whose torsional stiffness significantly varies depending on the subject's body size and gait speed [32]–[35]. Accordingly, we hypothesize that *SCKAFOs can replicate the biological spring-like function of the knee by implementing an accurately sized linear torsional spring during the stance phase and allowing for free knee motion during the swing phase of the gait*.

Researchers started investigating the use of elastic components in the design of orthoses and prostheses decades ago [36]–[38]. In early orthotic devices, the compliant components remained attached throughout the movement cycle. More recent research on assistive devices that incorporates compliance is primarily implemented in the design of prostheses [39], [40] and ankle orthoses [41]–[44]. Researchers have also designed underactuated exoskeletons that implement a spring in parallel with the knee in the stance phase of the gait [34], [35], [45]. However, these compliant devices provide a small percentage of the necessary knee quasi-stiffness (up to ∼20%) and are mostly designed to assist able-bodied subjects.

This paper presents the mechanical design and functional (i.e., nonclinical) evaluation of a quasi-passive compliant stance control orthosis (CSCO) that implements a linear spring in parallel with an impaired knee joint to compliantly support it during the stance phase, then allows the leg to freely swing to initiate the next step, as shown in Fig. 1. A preliminary conference paper version of this manuscript describes the basic design of the orthosis [46], with this paper greatly expanding on that by including the mechanical design analysis and characterization, control algorithm, and preliminary functional evaluation on three unimpaired volunteers, with performance compared to a commercial SCKAFO.

II. Device Design

A. Moment-Angle Behavior of Knee

Fig. 2-top schematically depicts the lower extremity limbs in a gait cycle, and Fig. 2-bottom shows a typical moment-angle cycle for an unimpaired knee during walking on level ground, with the corresponding gait instants labeled. The stance phase of walking is composed of a weight acceptance phase [first ∼40%, as depicted in Fig. 2(a)–(c)] and a stance termination phase [∼40%–63%, as shown in Fig. 2(c) and (d)] [32], [47]–[49]. During the weight acceptance phase, the knee undergoes substantial loads to support the weight of the superior limbs; therefore, it is highly prone to collapse without proper function of the musculature system or external assistance during this phase. As Fig. 2 shows and previous research suggests, the knee behaves close to a linear torsional spring in the weight-acceptance phase (particularly at the preferred gait speed). This spring stiffness is defined as *the slope of a linear fit to the moment-angle graph of the knee in this phase* [32], [33]. In our previous studies, we found that the knee quasi-stiffness in the weight acceptance phase can significantly vary depending on the user's body size and gait conditions demonstrating values up to ∼ $750\ \mathrm{N.m.rad^{-1}}$ for healthy adults during level ground walking

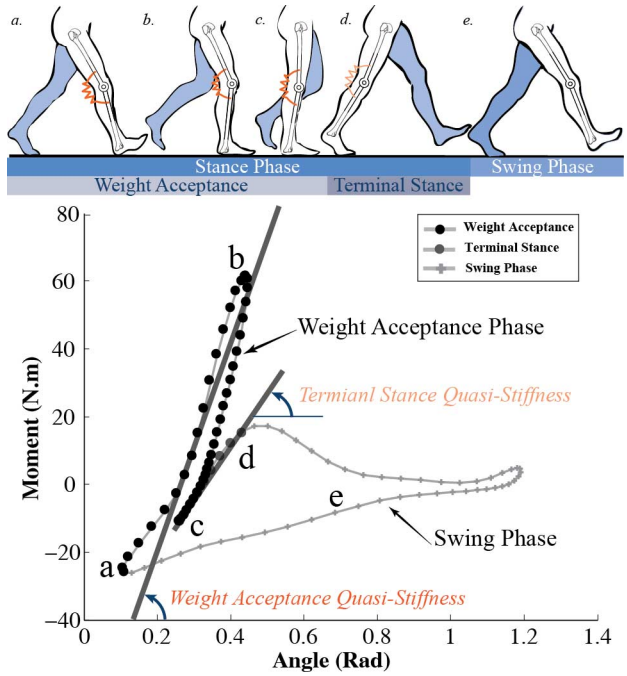

Fig. 2. Top: Schematic of lower extremity limbs during a gait cycle (schematic graphics adapted from [47]). Knee behaves close to a torsional spring in the weight acceptance phase of the gait as indicated. Bottom: Moment-angle graph for the knee of a subject walking at 1.25 $\mathrm{m.s^{-1}}$ (data from [33]). Slope of the linear fit to the graph in the weight acceptance phase is termed as the knee quasi-stiffness in this phase. Knee function can be replaced by a linear torsional spring with spring constant equal to the knee quasi-stiffness.

[32], [33]. The knee exhibits substantially smaller quasi-stiffness and moment during the terminal stance phase and remains nearly silent during the swing phase of the gait, [32], [48], [50]; implying a less eminent need for external stabilization.

In our previous work, we investigated the linear moment-angle behavior of the lower extremity joints. Particularly, we studied the effect of body size and gait speed on the knee moment-angle performance of subjects with gait speed of 1.01–2.63 $\mathrm{m.s^{-1}}$, body height of 1.43–1.86 m, and body weight of 56.0–94.0 kg [32], [33]. We showed that the human knee exhibits a stance excursion of 6° to 30°, quasi-stiffness of 80–750 $\mathrm{N.m.rad^{-1}}$, and moment of 45–105 N.m when walking on level ground [32]. We also showed that the angle of initiation of the weight acceptance phase (the angle at which the knee moment is zero) ranges from 6° to 32° and significantly varies depending on the weight carriage and gait speed [32]. The weight acceptance phase spans ∼40% of the gait which, depending on the gait speed and duration of the gait cycle, corresponds to a period of ∼400–500 ms assuming a cycle duration of ∼1–1.25 s.

B. Design Objectives

In order to approximate the linear moment-angle behavior of the knee, a compliant knee joint should engage a linear torsional spring (sized based on the body stature and gait conditions [32], [33]) in parallel with the knee at the onset of the stance phase and disengage it at the end of the weight acceptance phase to allow for free motion during the rest of the gait. Considering the biological performance of the human knee explained in the

previous section and extensive consultation we received from orthotists, we envision the following functional and safety requirements for the CSCO.

1) The knee joint stiffness of CSCO in stance should be sizable/selectable for a specific user depending on stature and gait conditions.
2) The CSCO should be capable of accommodating torsional stiffness of 80–750 $\mathrm{N.m.rad^{-1}}$ and maximum moment of up to 105 N.m.
3) We define the angular resolution of engagement as the smallest difference between the angles at which the orthosis can engage the spring. The CSCO should demonstrate high angular resolution (we target $\sim 1^\circ$) to be able to capture the knee motion in stance.
4) Adjustable angle of engagement/disengagement to capture the variable angle of initiation and termination of the weight acceptance phase, which ranges from 6° to 32° as observed for humans at different gait speeds and weight carriage conditions, as well as stair ascent/descent.
5) We define engagement/disengagement latency as the temporal duration between the electronic signal to the CSCO and corresponding engagement/disengagement of the spring. Theoretically the mechanism should exhibit instantaneous engagement/disengagement (researchers suggest 1% of the gait corresponding to $\sim$10 ms [17]) to be responsive at the onset and end of the weight acceptance phase.
6) The CSCO should demonstrate a joint excursion of 6° to 30° in the stance phase to capture the range of knee excursion observed for humans.
7) We define reliability as the percentage of cycles wherein the mechanism successfully engages/disengages the spring at the intended time. To avoid causing patients to fall and stumble, the CSCO should demonstrate 100% reliability of engagement/disengagement.
8) We define endurance as the number of the operation cycles that the orthosis can undergo before any mechanical or electrical failure occurs. We target 500 000 operation cycles, which is the number of operation cycles that the CSCO would experience in a six month period (as suggested by other researchers [17]).
9) The device should always allow the knee to extend so that the leg can quickly obtain an upright posture upon stumble and initiate a stable stance phase.
10) The device weight should be comparable to or lighter than available commercial SCKAFOs (we target $\sim$3 kg, which is the weight of SensorWalk from OttoBock).
11) We define the electric current demand as the average current the orthosis mechanism requires. The device should be capable of functioning for a whole day and require only a small battery. We envision an electric current demand of 300 mAh for the device so that it can function throughout a day using a battery with a capacity of 2500 mAh.
12) The CSCO should be capable of disengagement of a loaded spring to avoid causing wearers to stumble. This is particularly important when the user initiates the swing phase while the spring is still loaded. In this case, the CSCO should be able to disengage the spring; otherwise the knee would lock on the user and prevent foot clearance with the ground.
13) The engagement/disengagement control algorithm should not require the user to move to a particular kinematic configuration. Configuration-dependent engagement/disengagement can result in falling if the patient fails to move to the required configuration for engagement/disengagement; hence, it can heavily affect the performance of a stance control orthosis. The abovementioned design objectives for the CSCO are summarized in Table I. Since the CSCO is intended to be used for daily life activities, noise generation and cosmetic appearance should be appealing and favorably comparable with commercially available devices.

TABLE I
TARGET AND REALIZED VALUES FOR THE DESIGN PARAMETERS

Design Parameter	Target	Realized
Spring Sizablity	Yes	Yes
Joint Excursion in Stance (deg)	[6 to 30]	[0 , 40]
Angular Resolution (deg)	1	<1
Engagement Latency (ms)	10	30
Maximum Moment (N.m)	105	110
Torsional Stiffness ($\mathrm{N.m.rad^{-1}}$)	[80 to 750]	$\sim\infty$
Angle of Engagement (deg)	[0 , 32]	[0 , 60]
Weight(kg)	3	3
Endurance	500,000	>140,000
Electric Current Demand (mAh)	300	50
Reliability	100%	100%
Knee Extension Allowance	Always	Always
Disengagement under Load	Yes	Yes
Configuration-Independent Engagement	Yes	Yes

C. Description of the Quasi-Passive Compliant Stance Control Orthosis

The CSCO is composed of a compliant stance control module (CSCM) integrated into a regular KAFO (fabricated by Otto-Bock) that lacks a lateral knee joint, as shown in Fig. 1 and detailed in Fig. 3. The CSCM includes a uniaxial joint setup, which functions as the lateral joint of the CSCO, and a compliance control module (CCM) that exhibits two levels of stiffness through engagement/disengagement of a support spring, shown in Fig. 3. The lateral joint of the CSCO is primarily composed of a thigh chassis and a shank chassis as well as a pulley and additional structural components, as shown in Fig. 3. The CCM is assembled on the thigh and the pulley on the shank chassis. The CCM harnesses the shank chassis through a tendon attached to and wrapped around the pulley. The pulley rotates along with the knee joint, which, in turn, pulls the shaft of the CCM and compresses the return spring (and support spring, provided it is engaged). This transforms the linear stiffness of the CCM that is observed at the shaft to a torsional stiffness around the knee joint.

D. Compliance Control Module

The CCM is responsible for engaging and disengaging the support spring in parallel with the knee joint. The components of this module include a shaft, friction lever, bearing block, support spring, return spring, shock absorber, and engagement

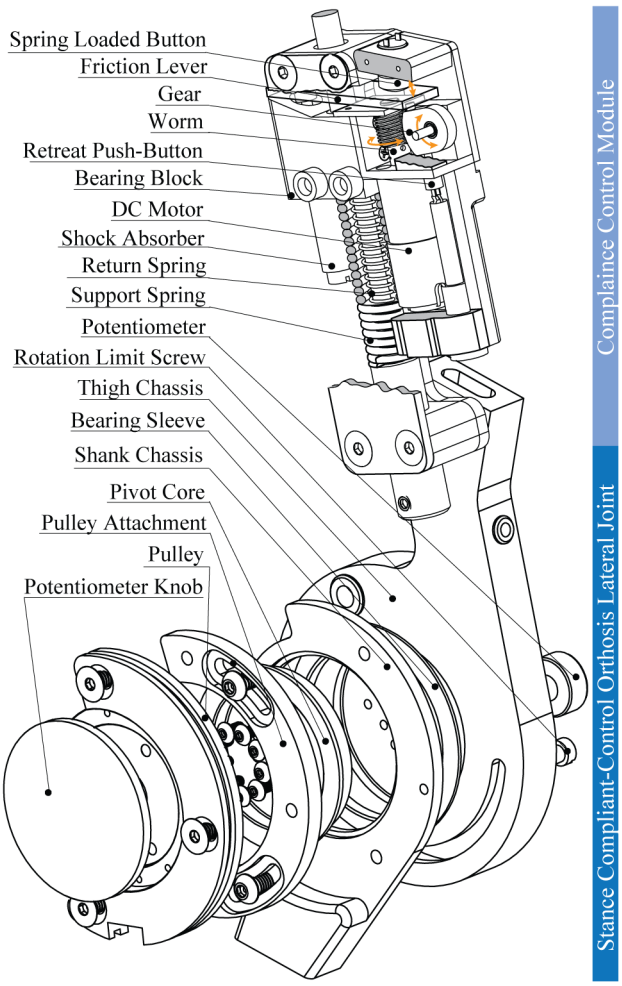

Fig. 3. Compliant stance control module is mainly composed of the CCM and the lateral joint of the stance control orthosis. CCM is mounted on the thigh chassis and harnesses the shank chassis using a tendon that is wrapped around the pulley. CCM engages the support spring during the weight acceptance phase (or the entire stance phase, depending on the user's gait requirements) to stabilize an affected knee, and disengages it during the rest of the gait to allow for free progression of the limb.

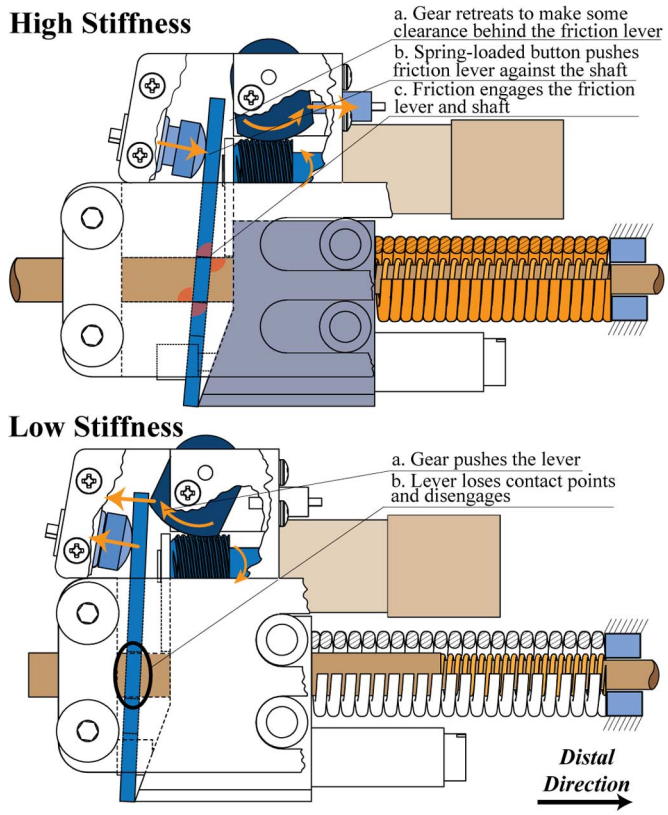

Fig. 4. Top: *Engagement of the support spring*. When the friction lever is engaged, flexion of the knee compresses both the return and support springs of the compliance control module, Bottom: *Disengagement of the support spring*. When the friction lever is disengaged, flexion of the knee only compresses the return spring (which is mainly incorporated to return the shaft in the extension period). Only those parts of the compliance control module that are involved in each mode are colored.

mechanism, as detailed in Fig. 3. The CCM exploits friction-based latching to engage the support spring in the stance phase, and disengage it during the rest of the gait. Friction-based latching has been utilized for prosthetic applications [51] as well as clamping purposes [52]. Here, the CCM uses a motor to drive a worm-gear set that, in combination with a spring-loaded push-button, brings a friction lever either in contact with the shaft to latch the bearing block to the shaft, or away from the shaft to unlatch the bearing block and allow for free motion of the shaft inside the bearing block. The engagement mechanism also includes a spring-loaded and a retreat push-button to provide the CSCO controller with feedback on the position of the friction lever. The sequence of steps for engagement and disengagement of the support spring is detailed here.

Engagement of the Support Spring: To engage the support spring, the worm-gear should spin counterclockwise to move the gear away from the friction lever and clear behind it. This movement terminates when the gear presses the retreat button, which sends a feedback signal to the controller to stop the motor, as shown in Fig. 4-top. The spring-loaded push-button presses the friction lever against the shaft to bring them in contact at the two points, as highlighted in Fig. 4-top. This introduces a small friction force on the friction lever at the contact points, which is transferred to the bearing block through the friction lever. The interaction force between the bearing block and the friction lever induces higher normal forces between the friction lever and the shaft, constituting a latching grip between the bearing block, shaft, and friction lever. As such, the bearing block moves along with the shaft and compresses the support spring. Since shaft movement always compresses the return spring, any distal force on the shaft (as a result of knee flexion, shown by an arrow on the shaft in Fig. 4-top) compresses both the return and support springs. Consequently, the CCM exhibits the summation of the stiffnesses of both springs along the shaft axis. A proximal force on the shaft (mainly applied by the return spring during knee extension) relaxes the friction forces on the friction lever at the contact points and releases the latching grip. Therefore, a latch only occurs in the flexion direction, and remains if the support spring is engaged and loaded to maintain the latching friction forces.

Disengagement of the Support Spring: To disengage the support spring, the worm should spin clockwise to move the gear towards the friction lever. The gear touches the friction lever and releases its latch with the shaft and moves until it presses the

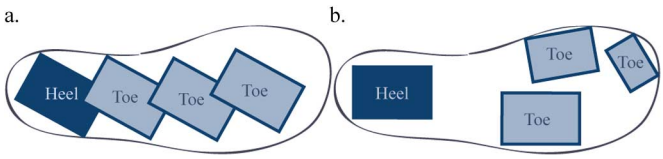

Fig. 5. Configuration of heel and toe sensors in the instrumented shoe insoles. Left: Linear configuration of force sensitive resistors (from OttoBock). Right: Ergonomic configuration of integrated conductive polymers (from B & L Engineering). Both insoles resulted in relatively similar performance for level ground and treadmill walking.

spring-loaded push-button after which a feedback signal is sent to the controller to stop the motor. One should notice that the forces applied on the lever by the gear and spring-loaded button generate a moment-couple that anchors the friction lever on the bearing block. Upon disengagement, the shaft freely slides inside the bearing block and friction lever without any force being transferred to the support spring. Accordingly, a distal force on the shaft only compresses the return spring. To allow free rotation in the swing phase, a relatively slack return spring should be chosen in order to only return the shaft to its original location after the swing phase without applying considerable assistive moment to the knee. The CCM also includes a shock absorber to dissipate any remaining energy, in case the support spring disengages while it is loaded.

E. Control Algorithm

The controller employs a finite state machine to engage and disengage the support spring. The controller identifies the gait phase by means of an instrumented shoe insole. We evaluated two types of foot sensors: a. A foot sensor with linear placement of force sensitive resistors from OttoBock, and b. A foot sensor with ergonomic placement of integrated conductive polymers from B & L Engineering, as shown in Fig. 5. We observed similar performance for the CSCO using both foot sensors, and we utilize the B & L insole for the remainder of this paper. The function of the CSCO is schematically depicted in Fig. 6-top. Fig. 6-middle approximately outlines the knee angular velocity, foot contact with the ground, and the status of the friction lever. Fig. 6-bottom shows the knee angle profile for a subject walking at 1.25 $\mathrm{m.s^{-1}}$ on level ground and the period during which the support spring is intended to be engaged and loaded. Fig. 7 describes the finite state machine that is implemented to control the CCM for walking on level ground. The states include the following.

1) *Weight Acceptance (WA)*: Either the heel sensor is on or both heel and toe sensors are on. The controller engages the support spring.
2) *Terminal Stance (TS)*: Any of the toe sensors are on and the heel is off. If the user can maintain stability during this phase, the CCM can disengage the support spring; otherwise, the support spring can remain engaged. The ability of the user to maintain stability can be evaluated by an orthotist/physician and programmed into the device.
3) *Swing (SW)*: The toe and heel sensors are off. The controller monitors the knee velocity direction during the swing phase to identify the flexion and extension period of knee excursion in the swing phase. The controller disengages the support spring during the flexion period of the swing phase and engages it during the extension period, as a precautionary measure against the mechanism's latching latency. Although the friction lever is engaged during the extension period of swing phase, the support spring is loaded because the engagement mechanism only initiates a latch in the flexion direction, as discussed in Section II-D.

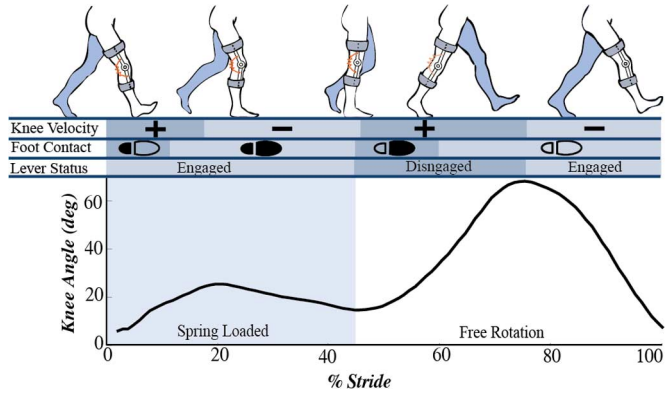

Fig. 6. Top: Device engages a spring in the weight acceptance phase of the gait (and potentially the terminal stance depending on the needs of the user). Middle: Statuses of the knee motion, heel and toe contact with the ground, and engagement of the friction lever. Bottom: Knee angle profile for a healthy subject walking with the gait speed of 1.25 $\mathrm{m.s^{-1}}$ (data from [33]).

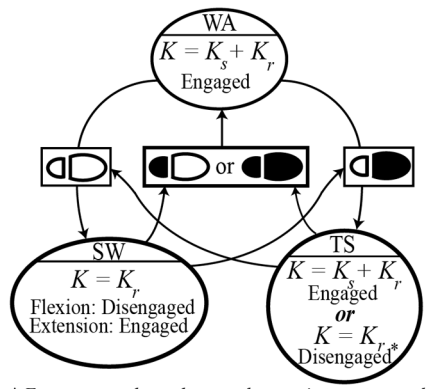

Fig. 7. Finite state machine used to control the stiffness of the compliance stance control module for level ground walking. Finite state machine includes three states: WA: weight acceptance, TS: terminal stance, and SW: swing phase. Transition between the state occurs when the status of foot contact with the ground changes. Each circle shows the stiffness of the compliance control module and status of the friction lever engagement.

We employed a Microcontroller MPC5534 from Freescale Semiconductor Co. (MPC5534EVBE) to implement the finite state machine for two CSCOs (left and right orthoses). The controller measures the knee angle using a rotary potentiometer (Model 357, Vishay Co.) that is integrated inside the orthosis pulley, and the knee velocity is obtained by differentiating the potentiometer signal. The controller identifies the status of the friction lever using the signals received from the push-buttons incorporated in the CCM. More specifically, the signal from the spring-loaded push-button defines if the friction lever is disengaged, while the signal from the retreat push-button defines

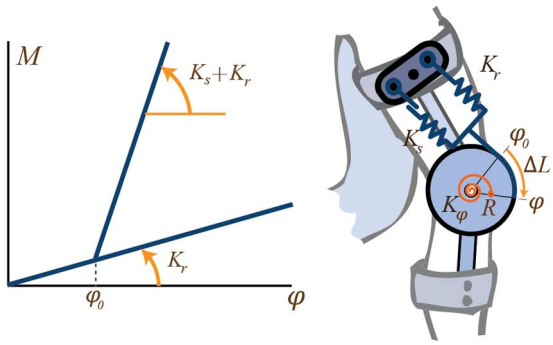

Fig. 8. Top: Schematic configuration of the return and support springs. Output stiffness of the compliance control module is the summation of the spring constants of both springs if the support spring is engaged, and only the spring constant of the return spring otherwise. Springs apply a force on the pulley with radius R. Effect of the linear return stiffness K_r and support stiffness K_s is experienced as an imaginary torsional spring around the center of the pulley with torsional stiffness K_φ.

if the friction lever is engaged. A serial-to-Bluetooth adapter (Wireless RS232, Willies Computer Software Co.) establishes wireless transfer of data to a host LabView module implemented on a computer for data collection. We used a dual H-Bridge from Solarobotics Co. to drive a Faulhaber 2024 dc Motor that we used in the design of the CCM. A battery pack with capacity of 2500 mAh powers the controller, orthosis and the wireless connection systems.

F. Design Analyses and Characterization

Moment-Angle Relationship: As discussed in Section II-C, the CSCO tendon is wrapped around and anchored to the pulley that is mounted on the shank chassis. When the knee flexes, the return spring (and support spring if engaged) will compress and apply a moment on the pulley, as schematically shown in Fig. 8-top. This moment can be calculated as

$$M = K_L \cdot \Delta L \cdot R \tag{1}$$

where R is the radius of the pulley and K_L is the linear stiffness of the CCM observed at the shaft. Also, a knee flexion of $\Delta\varphi$ results in a shaft movement of ΔL. Thus, the stiffness of an imaginary linear torsional spring K_φ that can replace the transformed stiffness CCM around the knee would be

$$K_\varphi = K_L \cdot \Delta L \cdot \frac{R}{\Delta\varphi}. \tag{2}$$

And since $\Delta L = R\Delta\varphi$, we conclude

$$K_\varphi = K_L \cdot R^2. \tag{3}$$

K_L is the stiffness of the return spring when the friction lever is disengaged and the summation of the stiffness of both springs when the support spring is engaged

$$K_L = \begin{cases} K_r + K_s, & \text{engaged} \\ K_r, & \text{disengaged} \end{cases}. \tag{4}$$

Combining (3) and (4) gives us

$$K_\varphi = \begin{cases} (K_r + K_s) \cdot R^2 & \text{engaged} \\ K_r \cdot R^2 & \text{disengaged} \end{cases}. \tag{5}$$

This suggests the following equation for the assistive moment observed at the knee joint:

$$M = \begin{cases} K_r \cdot R^2 \cdot \varphi + K_s \cdot R^2(\varphi - \varphi_0), & \text{engaged} \\ K_r \cdot R^2 \cdot \varphi, & \text{disengaged} \end{cases}. \tag{6}$$

Here, φ_0 is the angle at which the support spring is engaged. Fig. 8-bottom shows the theoretical moment-angle performance of the CSCO.

Sizing the Support Spring: An informed selection of the support spring can help the device implement a natural amount of compliance and minimize the compensatory movements of the body. Section II-A explains that the knee's function can be replaced by a torsional spring with a stiffness equal to the knee quasi-stiffness in the stance phase. In our previous works, we showed that a subject's knee and ankle quasi-stiffnesses significantly depend on body size and gait conditions [32], [53]. Current prosthetic design approaches usually employ the joint quasi-stiffness of healthy subjects with average weight and height, which requires substantial effort and time to conduct a gait lab study for each target user size, and additional tuning for the specific patient [40], [54], [55]. Alternatively, we proposed a series of statistical models that can estimate the quasi-stiffnesses of the knee and ankle joints in the stance phase of the gait relatively closely [33], [56]. Table II lists the most general and simplified forms of the statistical models that estimate the knee quasi-stiffness in the weight acceptance phase. The most general model tends to provide a closer estimation of the knee quasi-stiffness for a wide range of gait speed (1.01 *to* 2.63 ms^1), weight (67.7–94.0 kg), height (1.43–1.86 m), and knee excursion (6° to 28°), whereas the stature-based model estimates the knee quasi-stiffness only at the preferred gait speed and trades accuracy for simplicity by approximating the knee excursion and gait speed. Here, we exploit these statistical models to size the support spring of the device for users with complete impairment. For other users, the support spring stiffness can be a function of the level of impairment of the knee joint.

Friction Lever Dimensions: Fig. 9 shows the free body diagram of the friction lever. We assume that an initial moment around the point of contact between the lever and bearing block b (e.g., caused by the weight of the lever and the spring-loaded push-button) brings the friction lever in contact with the shaft at two points p and q. The interaction force between the lever and bearing block F_b, which is identical to the shaft force F, induces friction forces between the lever and shaft, F_p and F_q. Therefore, the normal friction forces are proportionate to the moment-arm around the center of the shaft r. Here, we derive a relationship between r, and the friction lever thickness t and diameter D under which the friction forces cause a latching grip between the shaft and friction lever.

The friction lever is stationary in the direction perpendicular to the shaft, therefore

$$\Sigma F_x = 0 \tag{7}$$

TABLE II
MODELS TO SIZE THE SUPPORT SPRING OF THE COMPLIANT STANCE CONTROL ORTHOSIS

Model	$K_s(\frac{Nm}{rad})$	$V(\frac{m}{s})$	$H(m)$	$W(kg)$	$\varphi(°)$
General Form	$K_s = \{69.8\,VHW - 112.8\,VW - 73.6\,WH + 192.0\,W - 4458\}/\varphi - \{1.37 - 0.52\,V\}WH + 264$	[1.01, 2.63]	[1.43, 1.86]	[67.7, 94.0]	[6, 28]
Stature-Based†	$K_s = 5.21\,W\sqrt{H^3} - 7.50\,W\sqrt{H} - 5.83\,WH + 11.64\,W - 6$	$1.097\sqrt{H}$	[1.43, 1.86]	[67.7, 94.0]	16.5

K_s: Stiffness of Support Spring V: Gait Speed H: User's Height φ: Knee Excursion in the Weight Acceptance Phase W: User's Weight
† To obtain the stature-based models, the general-form models are simplified for the approximated optimal gait speed of $V = 1.097\sqrt{H}$, and average knee excursion of $\varphi = 16.5°$ [33].

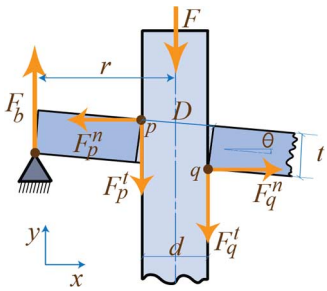

Fig. 9. Free body diagram of the friction lever under the interaction with the shaft and bearing block. The interaction force from the bearing block F_b generates normal forces between the friction lever and the shaft F_p^n and F_q^n; inducing tangential friction forces F_p^t and F_q^t. If the moment arm r is long enough, latching occurs and the shaft, friction lever, and bearing block lock together.

where F_x denotes any force applied on the friction lever along the x-axis. The normal contact forces at p and q (i.e., F_p^n and F_q^n) cause the tangential friction forces F_p^t and F_q^t on the friction lever. Expanding (7) concludes

$$F_p^n = F_q^n \tag{8}$$

which in turn implies that the friction forces are equal

$$F_p^t = F_q^t. \tag{9}$$

Since the lever is stationary around b, the summation of moments applied on the lever should be zero around this point

$$\Sigma M_b = 0 \tag{10}$$

where M_b stands for any moment applied on the friction lever around an axis passing through b and perpendicular to the plane of movement. Expanding (10) and including (9) gives us

$$F_p^n(D \cdot \sin\theta + t \cdot \cos\theta) - F_p^t(2r) = 0 \tag{11}$$

where D is the diameter of the hole of the friction lever, t is the thickness of the friction lever, and $\boldsymbol{\theta}$ is the tilt angle of the friction lever with respect to the x-axis. In order for the friction lever to engage with the shaft, the friction forces should remain lower than the maximum friction force

$$F_p^t \le F_p^n \cdot \mu \tag{12}$$

where $\boldsymbol{\mu}$ is the coefficient of friction between the shaft and lever. Applying (11) in (12) concludes

$$r \ge \frac{(D \cdot \sin\theta + t \cdot \cos\theta)}{2\mu}. \tag{13}$$

For small tilt angles (i.e., $\theta \sim 0$), (13) can be simplified to

$$r \ge \frac{t}{2\mu}. \tag{14}$$

Moreover, the maximum normal stress $(\sigma_{\max})$ imposed by the interaction forces between the friction lever and shaft should not exceed the material's yield strength (σ_Y)

$$|\sigma_{\max}| \le \frac{\sigma_Y}{S}. \tag{15}$$

Here, S is a safety factor. The maximum normal stress occurs at the outer surface of the friction lever between points b and p

$$\sigma_{\max} = \frac{3Fr}{w\,t^2} + \frac{F}{w\,t}\sqrt{9\left(\frac{r}{t}\right)^2 + 1} \tag{16}$$

where w is the width of the friction lever. Combining (15) and (16) concludes

$$\frac{3r}{t} + \sqrt{\left(\frac{3r}{t}\right)^2 + 1} \le \frac{3\,w\,t\,R\sigma_Y}{M_{\text{Knee}}S} \tag{17}$$

where M_{Knee} is the maximum knee moment that the device experiences. We have employed a steel shaft and friction lever with case hardness of Rockwell C60–C64, that theoretically exhibits a lubricated static coefficient of friction of 0.15 and yield strength of ~670 MPa. The shaft diameter is 9.525 mm (3/8 in and the lever thickness 3.175 mm (1/8 in). Considering a safety factor of 1.5 and M_{Knee} of 110 N.m, the bearing block contact point should be 20 mm away from the center of the shaft.

III. MECHANICAL AND FUNCTIONAL EVALUATION

We conducted three tests to evaluate/measure the reliability, latency and endurance of the CSCO, and also the kinematic performance of three healthy volunteers using the CSCO, including a comparison to a commercial SCKAFO (Sensor Walk by Otto Bock).

Preclinical Static Loading: We measured the moment-angle performance of the device and the maximum moment that the device can hold. We mounted the CSCM on a test bench and applied a series of moments under three levels of stiffness and three angles of engagement. For each condition, we recorded the flexion angle at which the CSCM was stabilized. Fig. 10 shows the results of the experiment wherein the device employed a return spring with linear stiffness of 5 N.mm^{-1} (equivalent to 13 N.m.rad^{-1}), and support springs with linear stiffnesses of: a) 92 N.mm^{-1} (equivalent to 239 N.m.rad^{-1}), b) 42 N.mm^{-1} (equivalent to 127 N.m.rad^{-1}), and c) 34 N.mm^{-1} (equivalent to 89 N.m.rad^{-1}). The moment-angle data for conditions

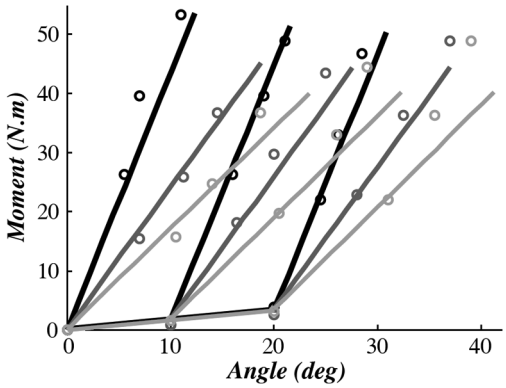

Fig. 10. Moment-angle characterization of the compliant stance control module using three different support springs: 239 $\mathrm{N.m.rad^{-1}}$ shown by black, 127 $\mathrm{N.m.rad^{-1}}$ shown by dark gray, and 89 $\mathrm{N.m.rad^{-1}}$ shown by light gray, and three different angle of engagement: 0°, 10°, and 20°. Experimental data are shown with circles and the theoretical data with solid lines. Stiffness of the return spring is 13 $\mathrm{N.m.rad^{-1}}$.

a, b, and c are shown with black, dark gray, and light gray, respectively. The experimental data are shown with circles and the theoretical data suggested by (6) with solid lines. Fig. 10 shows that (6) closely explains the moment-angle performance of the CSCM, especially at the low knee flexion values usually observed in walking. As dictated by the design objectives, we also applied moments of up to 110 N.m on the CSCM and found it able to tolerate them and hold its latch. The CSCM also functioned properly when the support spring was replaced with a solid cylinder (i.e., "rigid" joint).

Preclinical Dynamic Loading: We fabricated a mechanical knee simulator in order to evaluate the reliability and measure the latency of the CCM, as schematically shown in Fig. 11-top. The test machine consists of a four-bar linkage actuated by a large three-phase servomotor and servo controller (SGMAV-10A3A61 from Yaskawa and SGDV120AE from Omron Companies) [33], [57]. The servomotor follows the kinematic profile of the joint for which the module is being designed (here, the knee joint angle profile, taken from normative subject data [48]). The controller also sends a digital signal to the CCM to engage the support spring during the simulated stance phase and disengage during the rest of the gait, as shown in Fig. 11-bottom. The setup also records the feedback signals from the push-buttons embedded in the CCM to identify when the engagement/disengagement actually occurs. As discussed earlier, the mechanical system of the CCM imposes latency on the engagement/disengagement. The engagement latency (ΔT_e) and disengagement latency (ΔT_d) were estimated by measuring the time period between the command and feedback signals. We fabricated a prototype of the CCM and tested it on the knee joint simulator as schematically shown in Fig. 11-top. The prototype successfully underwent ∼30 000 gait cycles (with maximum moment of 60 Nm/rad) without any failure in the mechanical components and engagement. The average latencies for both engagement and disengagement were also measured using the test machine and reported to be ∼30 ms.

Preliminary Human Subjects Tests: We conducted a preliminary test on three healthy volunteers according to experimental protocols approved by the Institutional Review Board of Yale

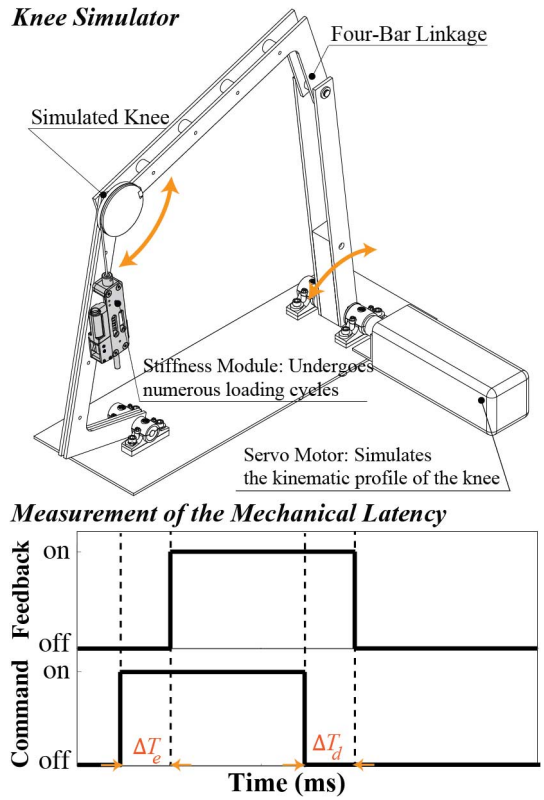

Fig. 11. Top: Knee simulator used to evaluate the mechanical function of the compliance control module and to measure the spring engagement/disengagement latency. Simulator is primarily a four-bar linkage mechanism driven by a servo motor. Compliance control module is mounted on the device and undergoes numerous working cycles. Bottom: Simulator controller sends an engagement command signal to the compliance control module and receives the feedback from the pushbuttons embedded in the module. Time differences between these signals indicate the mechanism engagement/disengagement latency.

University. Table III includes the demographic data of the volunteers as well as the preferred gait speeds of the trials. We compared the inter-subject mean kinematic profiles of the hip, knee, and ankle of the volunteers under compliant support provided by the CSCO with the rigid support provided by a SensorWalk commercial SCKAFO (OttoBock), which is likely the most advanced commercialized stance control orthosis. This device contains an electromechanical clutch at the knee that engages to lock the knee joint during the stance phase (sensed through an insole-based sensor), and releases the knee during swing.

The experiment included three conditions each consisting of 10 min of walking at the preferred gait speed according to the feedback obtained from the volunteers: 1) control condition (CC), 2) rigid support (RS), and 3) compliant support (CS). All conditions involved the device on the right leg of the volunteers, with no device on the left leg. The control condition consisted of the volunteers walking with a carbon-fiber jointed KAFO (i.e., free-swinging "pin" joint) without an active control module (the stance control modules of the SensorWalk and CSCO were assembled on the same KAFO, custom fit to the volunteers by a professional orthotist and fabricated by Otto Bock). The rigid support condition consisted of the volunteers walking with the SensorWalk device. For the compliant support condition, we

TABLE III
DEMOGRAPHIC DATA OF THE PARTICIPANTS AND TRIALS INFORMATION

No	Gender	Weight (*kg*)	Height (*cm*)	CC Speed ($^{m}/_{s}$)	CS Speed ($^{m}/_{s}$)	RS Speed ($^{m}/_{s}$)	Stiffness ($^{Nm}/_{rad}$)
1	M	71	178	1.00	1.00	1.00	240
2	M	70	170	0.90	0.90	0.75	240
3	M	74	169	0.90	0.90	0.80	240
	Mean	**73**	**172**	**0.93**	**0.93**	**0.85**	**240**
	SD	**2.6**	**4**	**0.06**	**0.06**	**0.13**	**0**

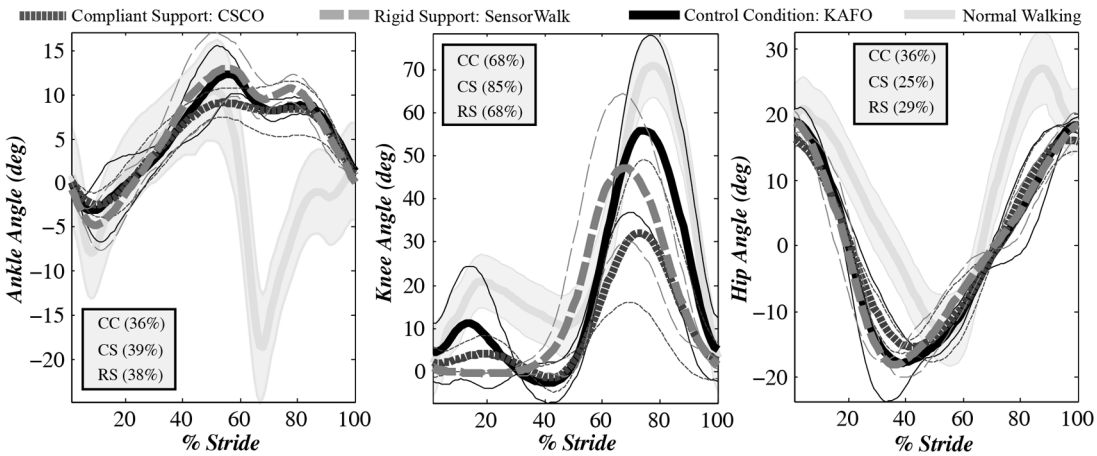

Fig. 12. Inter-subject mean angle profiles of the ankle, knee, and hip joints for three healthy volunteers walking at the preferred gait speed on a treadmill. CS: Volunteers walking with the CSCO with support spring stiffness of 240 $\mathrm{N.m.rad^{-1}}$, shown by black. RS: Volunteers walking with SensorWalk representing current stance control orthosis, shown by dark gray, and CC: Volunteers walking with the KAFO of SensorWalk/CSCO, shown by light gray. The figure also includes the normative angle profiles observed in average humans in normal walking [33], [56]. Thin lines show one standard deviation above and below the graphs.

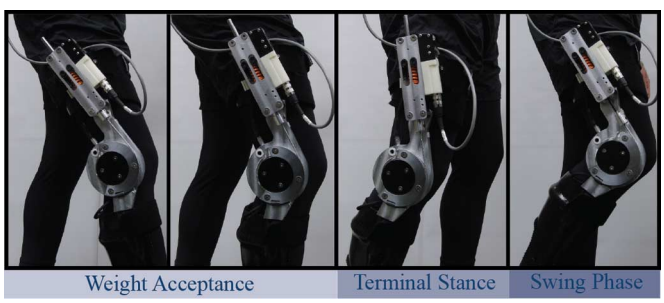

Fig. 13. High-speed image captures of the compliant stance control orthosis in a gait cycle of a healthy subject walking on a treadmill. Device compliantly supports the knee during the weight acceptance phase and liberates it during the rest of the gait.

replaced the stance control module of the SensorWalk with the CSCM. The equivalent support spring and return spring stiffnesses of the CSCM were chosen to be 240 $\mathrm{N.m.rad^{-1}}$ and 2 $\mathrm{N.m.rad^{-1}}$, respectively. To measure the joint angles, we placed a potentiometer at the knee and ankle of the devices and an instrumented orthopaedic goniometer (a potentiometer integrated in a goniometer from Elite Medical Instruments) at the hip joint of the volunteers. Fig. 12 illustrates the graphs of the inter-subject mean angles of hip, knee, and ankle by thicker traces as well as the lower and upper boundaries defined by the standard deviations with thinner traces. In this figure, black represents the results achieved by the CSCO, dark gray by the SensorWalk, and light gray by the jointed passive KAFO. The right heel strikes identified the beginning of the gait cycles. To give a sense of the repeatability of the traces over the entire gait period, the coefficients of variability (CV, described in [48]) of the mean profiles are also reported on each graph.

In order to compare the two Stance-Control Orthosis conditions (CSCO and SensorWalk), we calculated the common variance of correlation (R^2) and f-test p-value (p) between the joint angles when walking with those devices and when walking with the passive, jointed KAFO (control condition). We found R^2 values of 98%, 70%, and 98% for the ankle, knee, and hip angles, respectively, when walking with the SensorWalk, and R^2 values of 97%, 97%, and 98% when walking with the CSCO compared to walking with the KAFO as the baseline (as suggested by other researchers [58]), with $p < 0.0001$ for all profiles. Considering those values, the performance of our CSCO is closer to the control condition than the Sensor Walk, and especially so for the knee joint. These similarities and differences can also be qualitatively seen in the traces in Fig. 12.

As additional measures, we reported the preferred gait speed of the volunteers across all conditions. We found an average preferred speed of $\sim 0.93\ \mathrm{ms^{-1}}$ for the control and compliant support conditions, and $\sim 0.83\ \mathrm{ms^{-1}}$ for the rigid support condition, as reported in Table III. A sequence of high-speed image captures of the treadmill gait of one of the volunteers is also shown in Fig. 13.

IV. CONCLUSION AND FUTURE WORK

In this paper, we presented the mechanical design and functional evaluation of a quasi-passive CSCO that can compliantly

support the impaired or weak knee joint of a patient suffering from musculoskeletal disorders when walking on level ground. Inspired by the natural behavior of healthy human knees, the CSCO implements a spring in parallel with the knee joint to fully/partially replace the function of quadriceps in the stance phase, and liberates the knee joint in the swing phase to allow for free progression of the leg to initiate the next step. We further discussed the control algorithm developed to identify the gait phase and determine the engagement/disengagement of the orthosis support spring.

We conducted three experiments to ensure that the CSCO demonstrates proper reliability, latency, and durability, and also to ensure that the CSCO does not substantially affect gait kinematics. In the first set of tests, we applied static moments on the compliant stance control module (CSCM) of the CSCO and observed that the moment-angle behavior of the CSCM validates the theoretical characterization of the device. In the second set of tests, we evaluated the reliability, latency, and endurance of the CSCO on a testing machine over more than 30 000 working cycles. Finally, we conducted a preliminary human subjects test on three healthy volunteers using the CSCO, SensorWalk, and a control condition using the KAFO of the CSCO/SensorWalk. We found that the kinematic patterns of the volunteers remained relatively invariant during walking with the CSCO and relatively variant with SensorWalk, in comparison to those of the volunteers during walking with the KAFO as the baseline.

The design of the CSCO is based on the hypothesis that compliant support can be beneficial to subjects with an unimpaired hip and an impaired knee. Although our preliminary experiments show that the CSCO could provide biomechanical benefits to healthy subjects, statistical inference about the hypothesis requires substantial experiments including healthy and impaired subjects. Particularly, the experiments should include patients with neuromuscular deficits in order to determine to what extent compliant stance control can stabilize a fully/partially impaired knee. We have designed the CSCO for the same population targeted by current stance control orthoses. However, the CSCO should be tested on subjects with a variety of neuromuscular impairments to identify the population for whom the CSCO is most beneficial.

There are a number of follow-on directions from the described work that we will be addressing in the future. First and foremost, we will be testing the device on impaired volunteers in order to examine the performance in its intended use scenario. We are in the process of examining whether the device can help enable higher gait speed, longer walking distance/period, and lower energy expenditure compared with current SCKAFOs in a human subjects experiment on a series of impaired subjects (currently ongoing by the study researchers and clinical collaborators). In addition to further testing, we would like to improve a few aspects of the design of the CSCO, including more sophisticated heat treatment of the friction lever to improve the endurance of the CSCM, as well as making the device smaller and lighter by reducing the performance range during stance, which is currently over designed in terms of both range of motion (current $\sim 40^\circ$ reduced to $\sim 20^\circ$ observed in normal human walking) and knee torque (currently capable of 110 N.m, able to be reduced to around 50 N.m [47]).

ACKNOWLEDGMENT

The authors would like to thank J. Belter for his assistance with the conception and development of the stance control orthosis. The authors further thank G. Tatarliev, J. Kolmas, and N. Demas for their assistance in the development of the testing machines, mechanical components, and electronic equipment.

REFERENCES

[1] W. Robert and M. Leslvie, "A physiologic rationale for orthotic prescription in paraplegia," *Clin. Prosthet. Orthot.*, vol. 11, no. 2, pp. 66–73, 1987.
[2] E. A. Hurley, "Use of KAFOs for patients with cerebral vascular accident, traumatic brain injury, spinal cord injury," *J. Prosthet. Orthot.*, vol. 18, no. 7, pp. 199–201, 2006.
[3] M. K. Taylor, "KAFOs for patients with neuromuscular deficiencies," *J. Prosthet. Orthot.*, vol. 18, no. 7, pp. 202–203, 2006.
[4] J. E. Earl, S. J. Piazza, and J. Hertel, "The protonics knee brace unloads the quadriceps muscles in healthy subjects," *J. Athletic Train.*, vol. 39, no. 1, pp. 44–49, 2004.
[5] C. Slemenda, K. Brandt, D. Heilman, S. Mazzuca, E. Braunstein, B. Katz, and F. Wolinsky, "Quadriceps weakness and osteoarthritis of the knee," *Ann. Internal Med.*, vol. 127, no. 2, pp. 97–104, 1997.
[6] J. B. Redford, J. V. Basmajian, and P. Trautman, *Orthotics: Clinical Practice and Rehabilitation Technology*. New York: Churchill Livingstone, 1995.
[7] S. Irby, K. Bernhardt, and K. Kaufman, "Gait of stance control orthosis users: The dynamic knee brace system," *Prosthet. Orthot. Int.*, vol. 29, no. 3, pp. 269–282, 2005.
[8] S. Irby, K. Bernhardt, and K. Kaufman, "Gait changes over time in stance control orthosis users," *Prosthet. Orthot. Int.*, vol. 31, no. 4, pp. 353–361, 2007.
[9] B. Zacharias and A. Kannenberg, "Clinical benefits of stance control orthosis systems: An analysis of the scientific literature," *J. Prosthet. Orthot.*, vol. 24, no. 1, pp. 2–7, 2012.
[10] T. Yakimovich, E. Lemaire, and J. Kofman, "Engineering design review of stance-control knee-ankle-foot orthoses," *J. Rehabil. Res. Develop.*, vol. 46, no. 2, pp. 257–267, 2009.
[11] R. Waters, J. Campbell, L. Thomas, L. Hugos, and P. Davis, "Energy costs of walking in lower-extremity plaster casts," *J. Bone Joint Surg. Am.*, vol. 64, no. 6, pp. 896–899, 1982.
[12] S. Hwang, S. Kang, K. Cho, and Y. Kim, "Biomechanical effect of electromechanical knee-ankle-foot-orthosis on knee joint control in patients with poliomyelitis," *Med. Biol. Eng. Comput.*, vol. 46, no. 6, pp. 541–549, 2008.
[13] B. Phillips and H. Zhao, "Predictors of assistive technology abandonment," *Assist. Technol.*, vol. 5, no. 1, pp. 36–45, 1993.
[14] K. R. Kaufman, S. E. Irby, J. W. Mathewson, R. W. Wirta, and D. H. Sutherland, "Energy-efficient knee-ankle-foot orthosis: A case study," *J. Prosthet. Orthot.*, vol. 8, no. 3, pp. 79–85, 1996.
[15] A. A. Rasmussen, K. M. Smith, and D. L. Damiano, "Biomechanical evaluation of the combination of bilateral stance-control knee-ankle-foot orthoses and a reciprocating gait orthosis in an adult with a spinal cord injury," *J. Prosthet. Orthot.*, vol. 19, no. 2, pp. 42–47, 2007.
[16] T. Yakimovich, E. D. Lemaire, and J. Kofman, "Preliminary kinematic evaluation of a new stance-control knee-ankle-foot orthosis," *Clin. Biomechan.*, vol. 21, no. 10, pp. 1081–1089, 2006.
[17] T. Yakimovich, J. Kofman, and E. D. Lemaire, "Design and evaluation of a stance-control knee-ankle-foot orthosis knee joint," *IEEE Trans. Neural Syst. Rehabil. Eng.*, vol. 14, no. 3, pp. 361–369, Sep. 2006.
[18] P. Davis, T. Bach, and D. Pereira, "The effect of stance control orthoses on gait characteristics and energy expenditure in knee-ankle-foot orthosis users," *Prosthet. Orthot. Int.*, vol. 34, no. 2, pp. 206–215, 2010.
[19] A. Cullell, J. C. Moreno, E. Rocon, A. Forner-Cordero, and J. L. Pons, "Biologically based design of an actuator system for a knee-ankle-foot orthosis," *Mechan. Mach. Theory*, vol. 44, no. 4, pp. 860–872, 2009.
[20] A. McMillan, K. Kendrick, J. Michael, J. Aronson, and G. Horton, "Preliminary evidence for effectiveness of a stance control orthosis," *J. Prosthet. Orthot.*, vol. 16, no. 1, pp. 6–13, 2004.
[21] E. D. Lemaire, L. Goudreau, T. Yakimovich, and J. Kofman, "Angular-velocity control approach for stance-control orthoses," *IEEE Trans. Neural Syst. Rehabil. Eng.*, vol. 17, no. 5, pp. 497–503, Oct. 2009.
[22] K. Bernhardt, S. Irby, and K. Kaufman, "Consumer opinions of a stance control knee orthosis," *Prosthet. Orthot. Int.*, vol. 30, no. 3, pp. 246–256, 2006.

[23] A. Zissimopoulos, S. Fatone, and S. Gard, "Biomechanical and energetic effects of a stance-control orthotic knee joint," *J. Rehabil. Res. Develop.*, vol. 44, no. 4, pp. 503–513, 2007.
[24] A. M. Dollar and H. Herr, "Lower extremity exoskeletons and active orthoses: Challenges and state-of-the-art," *IEEE Trans. Robotics*, vol. 24, no. 1, pp. 144–158, Feb. 2008.
[25] R. Stein, F. Hayday, S. Chong, A. Thompson, R. Rolf, K. James, and G. Bell, "Speed and efficiency in walking and wheeling with novel stimulation and bracing systems after spinal cord injury: A case study," *Neuromodulation*, vol. 8, no. 4, pp. 264–271, 2005.
[26] J. M. Font-Llagunes, R. Pàmies-Vilà, J. Alonso, and U. Lugrís, "Simulation and design of an active orthosis for an incomplete spinal cord injured subject," *Procedia IUTAM*, vol. 2, pp. 68–81, 2011.
[27] Y. Tokuhara, O. Kameyama, T. Kubota, M. Matsuura, and R. Ogawa, "Biomechanical study of gait using an intelligent brace," *J. Orthopaed. Sci.*, vol. 5, no. 4, pp. 342–348, 2000.
[28] M. Arazpour, A. Chitsazan, M. Ahmadi Bani, G. Rouhi, F. Tabatabai Ghomshe, and S. W. Hutchins, "The effect of a knee ankle foot orthosis incorporating an active knee mechanism on gait of a person with poliomyelitis," *Prosthet. Orthot. Int.*, 2013.
[29] E. D. Lemaire, R. Samadi, L. Goudreau, and J. Kofman, "Mechanical and biomechanical analysis of a linear piston design for angular-velocity-based orthotic control," *J. Rehabil. Res. Develop.*, vol. 50, no. 1, pp. 43–52, 2013.
[30] S. Gard and D. Childress, "What determines the vertical displacement of the body during normal walking?," *J. Prosthet. Orthot.*, vol. 13, no. 3, pp. 64–67, 2001.
[31] R. J. Ratcliffe and K. G. Holt, "Low frequency shock absorption in human walking," *Gait Posture*, vol. 5, no. 2, pp. 93–100, 1997.
[32] K. Shamaei and A. M. Dollar, "On the mechanics of the knee during the stance phase of the gait," in *Proc. IEEE Int. Conf. Rehabil. Robot.*, Zurich, Switzerland, 2011, pp. 1–7.
[33] K. Shamaei, G. S. Sawicki, and A. M. Dollar, "Estimation of quasi-stiffness of the human knee in the stance phase of walking," *PLoS One*, vol. 8, no. 3, p. e59993, 2013.
[34] M. Cherry, D. Choi, K. Deng, S. Kota, and D. Ferris, "Design and fabrication of an elastic knee orthosis: Preliminary results," presented at the Int. Design Eng. Tech. Conf. Comput. Inf. Eng. Conf. , Philadelphia, PA, 2006.
[35] C. Walsh, K. Endo, and H. Herr, "A quasi-passive leg exoskeleton for load-carrying augmentation," *Int. J. Humanoid Robot.*, vol. 4, no. 3, pp. 487–506, 2007.
[36] J. Glancy, "Elastic-materials as a source of external power in orthotics—Preliminary-report," *Orthot. Prosthet.*, vol. 30, no. 1, pp. 13–21, 1976.
[37] P. Allard, M. Duhaime, P. Thiry, and G. Drouin, "Use of gait simulation in the evaluation of a spring-loaded knee-joint orthosis for Duchenne muscular-dystrophy patients," *Med. Biol. Eng. Comput.*, vol. 19, no. 2, pp. 165–170, 1981.
[38] L. Fisher and G. Judge, "Bouncy knee—A stance phase flex-extend knee unit," *Prosthet. Orthot. Int,*, vol. 9, no. 3, pp. 129–136, 1985.
[39] L. Marks and J. Michael, "Science, medicine, the future—Artificial limbs," *Br. Med. J.*, vol. 323, no. 7315, pp. 732–735, 2001.
[40] E. Martinez-Vilialpando and H. Herr, "Agonist-antagonist active knee prosthesis: A preliminary study in level-ground walking," *J. Rehabil. Res. Develop.*, vol. 46, no. 3, pp. 361–373, 2009.
[41] D. J. Farris and G. S. Sawicki, "Linking the mechanics and energetics of hopping with elastic ankle exoskeletons," *J. Appl. Physiol.*, vol. 113, no. 12, pp. 1862–1872, 2012.
[42] D. Ferris, Z. Bohra, J. Lukos, and C. Kinnaird, "Neuromechanical adaptation to hopping with an elastic ankle-foot orthosis," *J. Appl. Physiol.*, vol. 100, no. 1, pp. 163–170, 2006.
[43] M. Wiggin, G. Sawicki, and S. Collins, "An exoskeleton using controlled energy storage and release to aid ankle propulsion," in *Proc. IEEE Int. Conf. Rehabil. Robot.*, Zurich, Switzerland, 2011, pp. 1–5.
[44] D. J. J. Bregman, M. M. van der Krogt, V. de Groot, J. Harlaar, M. Wisse, and S. H. Collins, "The effect of ankle foot orthosis stiffness on the energy cost of walking: A simulation study," *Clin. Biomechan.*, vol. 26, no. 9, pp. 955–961, 2011.
[45] G. Elliott, G. S. Sawicki, A. Marecki, and H. Herr, "The biomechanics and energetics of human running using an elastic knee exoskeleton," in *Proc. IEEE Int. Conf. Rehabil. Robot.*, Seattle, 2013, pp. 1–6.
[46] K. Shamaei, N. Paul, and D. Aaron, "A quasi-passive compliant stance control knee-ankle-foot orthosis," in *Proc. IEEE Int. Conf. Rehabil. Robot.*, Seattle, WA, 2013, pp. 1–6.
[47] J. Rose and J. G. Gamble, *Human Walking*, 3rd ed. Philadelphia, PA: Lippincott Williams Wilkins, 2006.
[48] D. Winter, *The Biomechanics and Motor Control of Human Gait: Normal, Elderly and Pathological*, 2nd ed. Waterloo, ON, Canada: Univ. Waterloo Press, 1991.
[49] J. Perry, *Gait Analysis: Normal and Pathological Function*. Thorofare, NJ: SLACK, 1992.
[50] S. Mochon and T. McMahon, "Ballistic walking—An improved model," *Math. Biosci.*, vol. 52, no. 3, pp. 241–260, 1980.
[51] S. Collins and A. Kuo, "Recycling energy to restore impaired ankle function during human walking," *Plos One*, vol. 5, no. 2, p. e9307, 2010.
[52] J. A. Sorensen and L. Nebr, "Quick action bar clamp/spreader," Patent D333 602, 1991.
[53] K. Shamaei, M. Cenciarini, and A. M. Dollar, "On the mechanics of the ankle in the stance phase of the gait," in *Proc. Annu. Int. Conf. IEEE EMBS*, Boston, MA, 2011, pp. 8135–8140.
[54] J. Markowitz, P. Krishnaswamy, M. Eilenberg, K. Endo, C. Barnhart, and H. Herr, "Speed adaptation in a powered transtibial prosthesis controlled with a neuromuscular model," *Phil. Trans. R. Soc. B-Biol. Sci.*, vol. 366, no. 1570, pp. 1621–1631, 2011.
[55] F. Sup, A. Bohara, and M. Goldfarb, "Design and control of a powered transfemoral prosthesis," *Int. J. Robot. Res.*, vol. 27, no. 2, pp. 263–273, 2008.
[56] K. Shamaei, G. S. Sawicki., and A. M. Dollar, "Estimation of quasi-stiffness and propulsive work of the human ankle in the stance phase of walking," *PLoS One*, vol. 8, no. 3, p. e59935, 2013.
[57] G. Tatarliev, "Design of a knee simulator for testing orthoses under," in *Senior Project*. New Haven, CT, USA: Yale Univ., 2011.
[58] P. Kao, C. Lewis, and D. Ferris, "Invariant ankle moment patterns when walking with and without a robotic ankle exoskeleton," *J. Biomechan.*, vol. 43, no. 2, pp. 203–209, 2010.

Kamran Shamaei (S'13) received the B.S. degree in mechanical engineering from Iran University of Science and Technology, Tehran, Iran, in 2005, and the M.S. degree in mechanical engineering from ETH, Zurich, Switzerland, in 2009. He is currently a Ph.D. degree candidate at the School of Engineering and Applied Science, Yale University, New Haven, CT, USA.

His current research area includes design and development of orthoses and prostheses, medical robotics, and surgical technologies.

Paul C. Napolitano is on track to receive the ABET-accredited B.S. degree in mechanical engineering from Yale University, New Haven, CT, USA, in May 2015.

His current area of research is in medical device design, particularly orthotics and drug delivery.

Aaron M. Dollar (SM'13) received the B.S. degree in mechanical engineering from the University of Massachusetts, Amherst, MA, USA, and the S.M. and Ph.D. degrees in engineering sciences from Harvard University, Cambridge, MA, USA, and conducted two years of postdoctoral research at the MIT Media Lab, Cambridge, MA, USA.

He is the John J. Lee Assistant Professor of Mechanical Engineering and Materials Science at Yale University, New Haven, CT, USA. His research topics include human and robotic grasping and dexterous manipulation, mechanisms and machine design, and assistive and rehabilitation devices including upper-limb prosthetics and lower-limb orthoses.

Prof. Dollar is the recipient of the 2013 DARPA Young Faculty Award, 2011 AFOSR Young Investigator Award, the 2010 Technology Review TR35 Young Innovator Award, and the 2010 NSF CAREER Award.